Geoderma 423 (2022) 115963

Contents lists available at ScienceDirect

Geoderma

journal homepage: www.elsevier.com/locate/geoderma

Land use impacts on weathering, soil properties, and carbon storage in wet Andosols, Indonesia

Sastrika Anindita[a,*], Steven Sleutel[a], Dimitri Vandenberghe[b], Johan De Grave[b], Veerle Vandenhende[b], Peter Finke[a]

[a] Department of Environment, Ghent University, Coupure links 653, B-9000 Ghent, Belgium
[b] Department of Geology, Ghent University, Krijgslaan 281/S8, 9000 Ghent, Belgium

ARTICLE INFO

Handling Editor: Karen Vancampenhout

Keywords:
Land use change
Volcanic soils
Weathering
Soil properties
Organic carbon

ABSTRACT

We investigated changes in geochemical soil properties in response to deposition age and land use management over 30 – 50 years on tropical volcanic soils. Our purpose was to find out how weathering stage and land use interactively affect soil properties and organic carbon, and to check if phenoforms (management-related soil subtypes) exist within the genoforms (genetic soil types). Soil samples were taken at land uses that have been converted (pine forest and agricultural land) and a natural forest as the original land use. The results showed that pine forest soil displayed more intense weathering as indicated by higher values of three weathering indices. Intensive agricultural practices also improved soil chemical properties such as pH, exchangeable base cations, base saturation, and organic carbon stock leading to WRB-qualifier of "*eutric*" in cultivated soils, whereas the average of bulk density was relatively similar between forests and cultivated soils. Positive correlations were found between amorphous materials and Al_o, specific surface area, and micropore volume. Correlations between the content of short-range order Al (hydr-) oxides (indicated by Al_o) and organic carbon were found in pine forest and agricultural soils, particularly in subsoils. Our results clearly indicate the increase of base cations retention due to less acidification and an increase of organic carbon stock under agricultural land use, likely due to stabilization with non-crystalline materials.

1. Introduction

Soil weathering is an essential process in order to understand soil formation and its interaction with the environment (Birkeland, 1999). This process can affect physical and chemical soil properties, storage of nutrients, and carbon. Volcanic ash soils generally weather following a sequence from primary minerals to short-range order (SRO) minerals, halloysite, and kaolinite (Parfitt et al., 1983). The rates of weathering from primary to secondary minerals depend on environmental conditions. Humid climate can enhance desilication and loss of base cations (Chadwick et al., 2003). Land use can modify the fate of weatherable minerals by serving as H^+ sink (Acid Neutralizing Capacity; Van Breemen et al., 1983) and by physical weathering, such as tillage (Wei et al., 2006).

Volcanic soils are susceptible to land use change, especially conversion to cultivated land, due to their inherent good chemical fertility. In cropland management, soil tillage creates a warmer and dryer soil climate and disrupts aggregates, which increases organic matter (OM) turnover (Bandyopadhyay, 2019) and enhances the chemical weathering (Li et al., 2021). Converting forest area to cropland in which tillage is practiced may affect Andosols, and thus deserves attention because of their fertility and intense agricultural use. Several studies reported negative effects such as disturbance of the geochemical cycle and less Organic Carbon (OC) storage (Lemenih et al., 2005; Sosnowska, 2012). However, manure application under agricultural management can increase soil OC stocks (Maillard and Angers, 2014). The conversion to cropland was reported to improve soil chemical properties such as the increase of K, Ca, Mg (Asio et al., 1999), but in contrast net acidification may also occur if nutrient export by harvesting is not compensated (Van Breemen et al., 1983).

The formation of SRO aluminosilicate materials, Fe oxide, and accumulation of OM are the main pedogenic processes in allophanic Andosols (Shoji et al., 1993). Interactions between nano-sized SRO minerals and soil OM play a significant role in the retention and

* Corresponding author at: Current address: Department of Environment, Ghent university, Coupure links 653, B-9000 Ghent Belgium.
E-mail address: sastrika.anindita@ugent.be (S. Anindita).

https://doi.org/10.1016/j.geoderma.2022.115963
Received 10 December 2020; Received in revised form 3 May 2022; Accepted 25 May 2022
Available online 3 June 2022

stabilization of carbon (Basile-Doelsch et al., 2015; Kleber et al., 2015; Lehmann and Kleber, 2015; Tamrat et al., 2019). Their presence also contribute to unique chemical and physical soil properties in Andosols, such as variable charge, low bulk density, high water holding capacity, and formation of stable soil aggregates. There is still no decisive information related to how weathering and geochemical properties are driven by land use in these soils.

Here, we investigated the change of geochemical soil properties as impacted by land use in Andosols from the Sunda volcanic arc region (Mt. Tangkuban Parahu and Mt. Burangrang), West Java, Indonesia. In particular, we tested the assumption that phenoforms (management-related soil subtypes) exist within the more general genoforms (genetic soil types; Droogers and Bouma, 1997; Rossiter and Bouma, 2018) of these specific Andosols. By analyzing their weathering statuses both geochemically and mineralogically, and OC contents, we aim at testing our assumption about age and parent materials, relating weathering, land use, and OC status.

2. Materials and methods

2.1. Environmental setting

The study areas were situated in the Mount Tangkuban Perahu and Mount Burangrang regions, which are part of the Sunda Volcanic Complex (SVC) in West Java, Indonesia (Fig. 1). Mt. Tangkuban Perahu is an active stratovolcano that was formed in the eastern rim caldera of ancient Mt. Sunda. Over the last 10,000 years, the dominant type of Tangkuban Perahu eruption is small scale phreatic. Only in 1910 there was a magmatic eruption affecting a small area with ejected volcanic ash and scoria rock. Mt. Burangrang is also part of the remaining Mt. Sunda, but is situated in the western part of the caldera rim and has older volcanic edifices (Silitonga, 1973). Soils in these areas were derived from similar parent material (basaltic-andesitic (ash) tuff), which originated from Holocene to Late Pleistocene activity (Dam et al., 1996; BBSDLP, 2017). The soil type was classified as Typic hapludands based on the soil map scale 1:50,000 (BBSDLP, 2017). The areas have a mean annual precipitation of 2000 – 3000 mm year^{-1} and mean annual

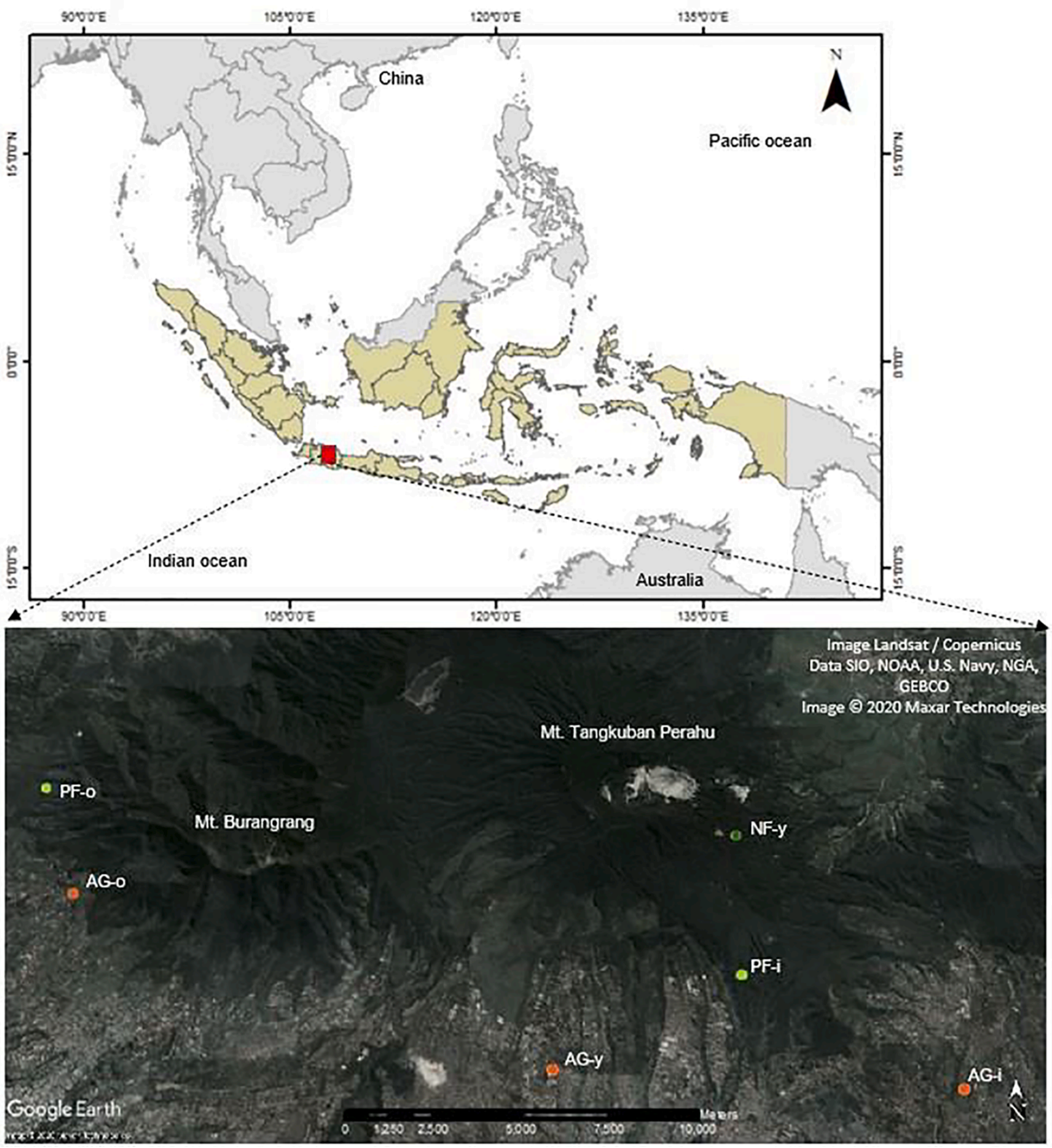

Fig. 1. Location of the study area and sampling sites.

temperature around 19–21 °C.

The study areas were located in deposits of different lithology and age i.e. Qyd (young deposition age), Qyt (intermediate deposition age), Qvu (old deposition age) (Silitonga, 1973) (Table 1; Fig. 2). Soil samples taken from Qyd and Qyt were located in Lembang district near Mt. Tangkuban Perahu. The radiocarbon dating of buried organic horizon in the Lembang district yielded age 8700 ± 200 and 14500 ± 300 yrs BP for 2A and 3A horizons, respectively (Chartres and Van Reuler, 1985). Soil samples from Qvu were located near Mt. Burangrang, in the border of Cisarua district. The maximum age of volcanic ash in this area was expected to be 10,000 yrs (Utami et al., 2019).

Most of the areas were under forest before 1900 but have been gradually opened since 18th century and subjected to high anthropic pressures. Currently, the primary forest occupies only the upper slopes within a distance of around 1 km surrounding the crater of Mt. Tangkuban Perahu. Other land uses such as pine forest is a secondary forest planted in 1962 for restoration purposes (Perhutani, 2014). Agricultural practices date back 30 – 50 years and involve mainly rotations of horticultural crops. The history of land use and management was obtained by collecting data from historical land use maps, queries to government institutions, and interviews with landowners (Table 1).

Table 1
Location of sampling sites, land use, slope, altitude, and age of soils.

Coordinates	Slope ()	Elevation (m)	Present vegetation and management	Land use history	Parent material	
					Lithology[b]	Approximate age (yrs)[c]
Primary forest (NF-y)[a]						
646′15.69″S 10737′21.98″E	15	1710	*Altingia excels, Schima wallichii, Astronia spectabilis, Castanopsis argenta, Quercus spp,*	Natural forest	Qyd (phase C-young eruption)	Holocene max. 8700 ± 200
Agricultural land (AG-y)						
648′9.00″S 10735′47.60″E	15	1313	- Annual crops: tomatoes, cabbage, broccoli, chilly Three crops rotation per year Intensive tillage Fertilizer: (1) mix of chicken, cow manure and rice husk = ±76 Mg/ha/year (2) inorganic fertilizer = 307 kg N ha^{-1}, 307 kg P ha^{-1}, 307 kg K ha^{-1}	- 1909–1917: degraded forest (shrub) (Topographical Service Batavia, 1941) Ca. 1940–1950: Unmanaged plantation (possibly coffee).Ca. 1970: Intensive cultivation (horticulture)	Qyd (phase C-young eruption)	Holocene max. 8700 ± 200
Pine forest (PF-i)						
647′54.80″S 10737′21.50″E	18	1343	- *Pinus merkusii* No fertilizer	- < 1900: Degraded (Dutch colonial era: wood production)Ca. 1960: Pine forest (production forest, pine sap/resin capture, locally coffee; agro forestry) . Ca. 2007: protected forest	Qyt (phase A-old eruption)	Holocene max. 8700 ± 200
Agricultural land (AG-i)						
648′48.60″S 10738′30.30″E	16	1163	- Annual crops: potatoes, broccoli, cabbage Max. three crops rotation per year Intensive tillage Fertilizer: (1) mix of chicken manure and rice husk = ± 20 Mg/ha/year (2) inorganic fertilizer = 144 kg N ha^{-1}, 144 kg P ha^{-1}, 144 kg K ha^{-1} as NPK fertilizer	- 1909–1917: Bamboo forest (Topographical Service Batavia, 1941)1940-ca.1980: unmanaged plantation, possibly coffee.Ca. 1980: Intensive cultivation (horticulture)	Qyt (phase A-old eruption)	Holocene max. 8700 ± 200
Pine forest (PF-o)						
645′38.50″S 10731′3.00″E	18	1128	- *Pinus merkusii* No fertilizer	- < 1900: Degraded (Dutch colonial era: wood production) Ca. 1960: conversion to pine forest. Previously and locally, pine trees with horticulture for 5 years, then agroforestry of pine trees with coffee, but because of low production, change to protected forest locally for tourism.	Qvu	Holocene 10,000
Agricultural land (AG-o)						
646′26.80″S 10731′20.30″E	14	1132	- Annual crops: chayote, cabbage, green bean One or two crops rotation per year Fertilizer: (1) mix of chicken manure and rice husk = ± 18 Mg/ha/year (2) inorganic fertilizer = 90 kg N ha^{-1}, 90 kg P ha^{-1}, 90 kg K ha^{-1}	- 1909–1917: Degraded forest (Topographical Service Batavia, 1941)1940-ca.1988: Conversion to unmanaged coffee plantation.Ca.1988: Cultivation (horticulture)	Qvu	Holocene 10,000

[a] -y: young soil age; -i: intermediate soil age; -o: old soil age.

[b] Based on Silitonga (1973). Qyd is defined as brownish sandy tuff from Mt. Dano and Mt. Tangkuban Parahu (eruption "C"; Van Bemmelen (1934)), which is very porous and contains very coarse hornblende crystals as well as lahar deposit, lapilli layers, and breccia; Qyt is tuffaceous sand with lapilli, bombs, scoriaceous lava, angular fragments of dense andesite-basalt, and many pumice fragments, mostly from Mt. Tangkuban Perahu (eruption "A"; Van Bemmelen (1934)) and Mt. Tampomas; Qvu is undifferentiated old volcanic product consist of volcanic breccia, lahar deposit and repeated interlayer lava. The eruption of phase A has older formation than the eruption of phase C (Arifin, 1994; Van Bemmelen, 1949).

[c] Based on (Chartres and Van Reuler, 1985; Kartadinata et al., 2002; Sunardy and Kimura, 1998; Utami et al., 2019).

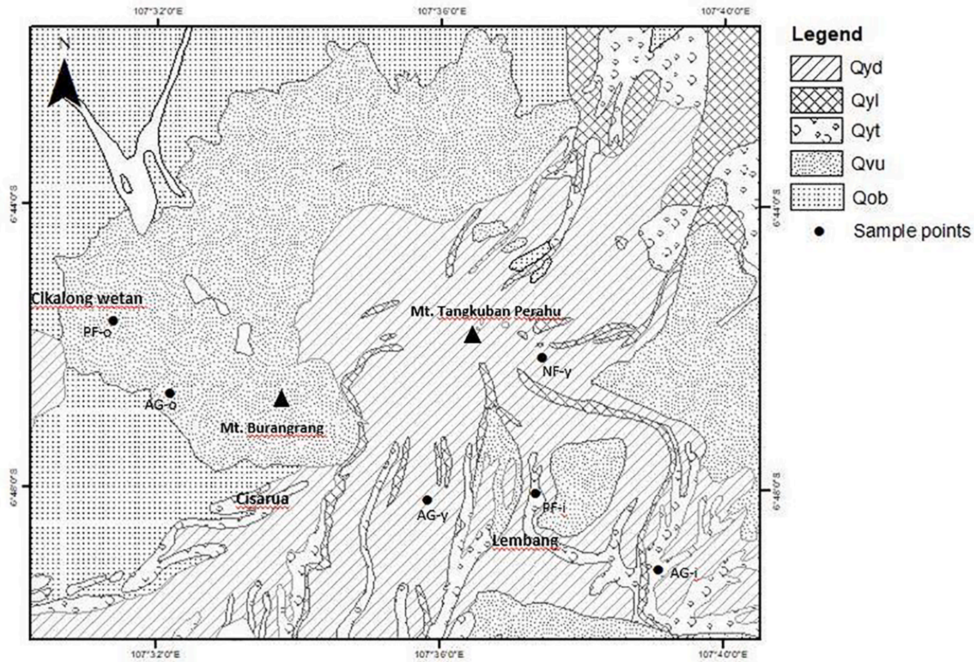

Fig. 2. Lithology map of studied soils.

2.2. Site description and soil sampling

We sampled an anthropo-chronosequence of volcanic soils in the Mt. Tangkuban Perahu and Mt. Burangrang, representing deposition materials age and land use histories as known from geological and historical land use maps. Six sites representing different land use (i.e. primary forest, pine forest, agricultural land) and lithology (i.e. Qyd, Qyt, Qvu) were selected. In Qyd, land use encompasses primary forest (NF-y) and agricultural fields (AG-y). The sites of Qyt and Qvu age both involve pine forest (PF-i, PF-o) and agricultural plots (AG-i, AG-o). All the sampling sites were situated on slopes near ± 17° and the agricultural sites were under terrace. Bulk undisturbed and disturbed core samples were taken from the topsoils (at 0 – 20, 20 – 40 cm) and the subsoils (±60 – 80 cm) in all sites. At each depth, the bulk samples were mixed thoroughly into composite samples.

2.3. Physico-chemical analyses

Selected physical and chemical soil analyses were used to compare soil characteristics among land use and deposition age. All analyses were made on air-dried fine earth (<2- mm) and the fraction > 2 mm was accounted as coarse fragments. Bulk density was measured on undisturbed samples taken at field-moist condition using the core method (Blake and Hartge, 1986). Particle size analysis was achieved after sonication, dispersion with Na^+ resin, and raising the pH until 8 – 9 without any pretreatment with H_2O_2 oxidation of organic matter (Bartoli et al., 1991; Delvaux et al., 1989; Rouiller et al., 1972). After full dispersion, the contents of sand, silt, and clay were determined by the pipet method. The pH was measured both in H_2O and 1 M KCl with a glass electrode pH meter at 1:5 and 1:2.5 soil:solution ratios, respectively. The total cation exchange capacity (CEC_T) and cations present on the exchange complex were determined using the compulsive exchange method at pH ± 4.1 – 5.3 (Gillman and Sumpter, 1986). Phosphate retention was analyzed following method by Blakemore et al. (1981). Total carbon contents were measured on bulk soil < 2 mm samples by the dry combustion method at 1100 – 1450 °C using LECO 928 series carbon/nitrogen analyzer. Total carbon corresponded to OC due to the absence of carbonates.

2.4. Selective extraction data

Selective dissolution was used to estimate levels of SRO minerals, and -metal-humus complexes. Sodium dithionite-citrate-bicarbonate (DCB) was used to extract free iron (Fe_d) (Mehra and Jackson, 1958). Sodium pyrophosphate extracted (Fe, Al)-humus complexes (Al_p, Fe_p) (McKeague, 1967). Silicon, aluminum, and iron extractable by dark ammonium oxalate (Al_o, Fe_o, Si_o) were used to estimate allophanic substances and ferrihydrite. Estimating OC bound onto SRO Fe oxide was done by extraction OC and Fe (Fe_h) with hydroxylamine hydrochloride ($NH_2OH.HCl$), after removing aqueous OC with deionized water. In the various extracts, Si, Al, and Fe concentrations were determined by ICP-OESn. The OC concentration of the $NH_2OH.HCl$ extracts was determined with a FORMACS$^{HT/TN-I}$ TOC-analyser (Skalar, The Netherlands).

2.5. Total elemental analysis and quantification of minerals

Major elements (Si, Al, Fe, Ti, Ca, Mg, K, Na, Mn, P) were measured by ICP-OES Varian 720-ES following the ISO14869-2 procedure. The weathering indices were derived from computing the molar ratios (SiO_2 / (Al_2O_3 + Fe_2O_3 + TiO_2) (Birkeland, 1999), (K + Ca)/Ti (Harrington and Whitney, 1987), the chemical index of alteration (CIA = 100% *Al_2O_3/(Al_2O_3 + CaO + Na_2O + K_2O) (Nesbitt and Young, 1982), and the total reserve in bases (TRB), which sums up the concentrations of alkaline and alkaline-earth cations, thus representing both their non-exchangeable and exchangeable pools (Herbillon, 1986). Acid-neutralizing capacity (ANC) was calculated at pH reference 3 following Brahy et al. (2000):

$$ANC = TRB + 6(Al_2O_3) + 6(Fe_2O_{3tot} - Fe_2O_{3d}) \quad (1)$$

Where TRB is expressed as 2(CaO) + 2(MgO) + 2(K_2O) + 2(Na_2O) and 6(Fe_2O_{3tot} – Fe_2O_{3d}) reflects Fe_2O_3 content of Fe-bearing silicates.

Identification and semi-quantification of minerals in the bulk soil (<2 mm) was done using X-ray diffraction (XRD) after removing OC with sodium hypochlorite (Anderson, 1961). The samples were pulverized until all grains passed a 500 μm mesh sieve. For each sample, a 2 g sub-sample was mixed with 20% zincite as internal standard and further micronized (grain size of 10 μm or less) by wet grinding with ethanol using a McCrone Micronizing mill. The obtained slurry was dried to obtain a powder for XRD analysis with a Bruker D8 ECO Advance apparatus, equipped with a Cu-anode (40 kV, 25 mA) and an energy-dispersive position sensitive LynxEye XE detector. The incoming beam was collimated to a fixed beam length of 17 mm. Phases were identified using the DIFFRAC.EVA suite. The spectra were interpreted semi quantitatively using the BGMN Rietveld method with Profex version 4.0 as user interface (Bergmann et al., 1998; Doebelin and Kleeberg, 2015). The amount of amorphous material was estimated from the mismatch between the obtained and the real amount of internal standard (20% of zincite).

2.6. Soil specific surface area

The specific surface area (SSA) was assessed on samples (<2 mm), first cleared of OM with 6% H_2O_2 at 80 °C, then dried at 100 °C under vacuum, from N_2 adsorption–desorption at 77°K using a Micromeristics Tristar I following the Brunauer–Emmet–Teller (BET) approach. Furthermore, the SSA of micropores was evaluated using t-plot analysis (Sing et al., 1985) as discussed earlier by Mayer and Xing (2001).

2.7. Statistical analysis

Statistical data analysis was done using IBM SPSS Statistics for Windows, version 27 (IBM Corp., Armonk, N.Y., USA). Means of the land-use groups or soil deposition ages were compared by ANOVA and the relations between geochemical soil properties was done by Pearson correlation. The non-parametric test was used if the data were not normally distributed or if the condition of homoscedasticity was unmet.

3. Results

3.1. Soil morphology

The pedons consist of A, AB, and Bw horizons followed by a lithologic discontinuity (i.e horizon 2AB) indicated by darker soil color than the above soil horizon. Soils are deep (>150 cm), well drained, and non-sticky. Field assessment of texture indicated little clay, but high sand and silt content. Distinct features occurred in forest sites which had ectorganic layers, dark black surface soil horizons (i.e horizon Ah), and concentration of boulders at depth 84–118 cm at site NF-y (Supplementary 1).

3.2. Soil physiochemical properties

Major physical and chemical soil properties are presented in Table 2. The bulk density was invariably below 0.8 g cm^{-3} in all soil horizons, which had P-retention ≥ 85%, except in NF-y (A, AB), PF-i (A1), AG-y and AG-i (Ap1). The pH_{H2O} was acidic ranging from 4.08 to 5.91 and did not follow distinct depth gradients. The pH_{KCl} was mostly below 5 and was associated with KCl-extractable aluminum (Al_{KCl}) contents which increases with the decrease of pH_{KCl}. Delta pH values (pH_{H2O} – pH_{KCl}) in sites NF-y and PF-o were < 0.5, indicating the dominance of variable charge constituents while other sites had delta pH ± 0.5 – 1.0 which may denote either a large dominance of variable charge or a mix (Uehara and Gillman, 1981). Soil pH_{H2O} and pH_{KCl} were higher in the cultivated soils than in forest soils ($p < 0.05$), coinciding with higher contents of base cations. Exchangeable Ca was the dominant base cation in all soils followed by Mg, K, and Na. Base saturation in cultivated soils (>100%) was higher than that under pine forest (<45%) and primary forest (<5%) ($p < 0.05$). Low amounts of exchangeable basic cations in forest soils were accompanied with substantial Al_{KCl} levels, as expected from pH_{KCl} values below 4.7. In all soils, the CEC_T was generally low regardless of land use (5.6 – 10.7 $cmol_{(+)}$ kg^{-1}) and was higher in topsoil than in subsoil ($p < 0.05$). Using the WRB textural classes (IUSS, 2015), texture is clay in all soil horizons (clay content = 47 – 71%), except in NF-y, A-AB-Bw (loam), AG-i, Ap1 (loam) and Ap2 (silty clay loam). The OC concentration was clearly higher in the topsoil (0–20 cm), viz. 23.6 – 54.4 g kg^{-1}, and decreased with depth in all studied soil profiles ($p < 0.05$). In subsoil, the OC concentration at pine forest soils and cultivated soils was lower than that in soils under primary forest. In the latter case, OC concentration was higher than in the corresponding agricultural soil. In pine forest soils, however, OC concentration was invariably lower than that in cultivates soils. Volcanic glass was observed in all studied soils and ranged between 0.1 and 5.4% by grain count.

3.3. Selective extraction data

Selective extraction data are presented in Table 2. The sum $Al_o + 1/2Fe_o$ was above 2% in all soil horizons, except in the topsoil of the NF-y (A, AB) and PF-i (A1, A2), and in subsoil AG-o (Bw), thus all pedons have at least one layer with andic properties. Oxalate extractable Si (Si_o) was detected but in small amounts ($Si_o \leq 3$ g kg^{-1}), suggesting the virtual absence of allophanic substances in most soil horizons of NF-y, AG-y, PF-i, AG-o, and PF-o pedons ($Si_o \leq 2.2$ g kg^{-1}), particularly in NF-y ($Si_o \leq 0.15$ g kg^{-1}). These constituents were detected in higher amounts in soil horizons of AG-i ($Si_o = 2.2$ – 3 g kg^{-1}). Oxalate extractable Al (Al_o) ranged from 2.3 to 36 g kg^{-1}. NF-y largely differed from other pedons with Al_o concentrations below 5 g kg^{-1}, while AG-i was set apart by the highest levels (31 – 36 g kg^{-1}). In older deposits, Al_o concentration was higher in the forest soil (26 – 28 g kg^{-1}) than in the cultivated soil AG-o (9 – 17 g kg^{-1}). In contrast, in other cultivated soils, Al_o was markedly higher (AG-y: 14 – 22 g kg^{-1}; AG-i: 31 – 36 g kg^{-1}) than in their respective forest counterparts (PF-i: 8 – 13 g kg^{-1}; PF-o: 25 – 28 g kg^{-1}). Allophane and imogolite were only detected in the pedons AG-i and PF-o (1 – 2 %). Pyrophosphate extractable Al (Al_p) concentrations ranged from 3.4 to 41 g kg^{-1}, denoting the importance of Al forms associated with OM. The Al_p/Al_o ratio was above 1 in NF-y (AB), AG-y (Ap 1–2), PF-i (A1-2), and AG-o (Bw). Oxalate extractable Fe (Fe_o) was present from 7.7 to 52 g kg^{-1}. The Fe_o/Fe_d ratio was large in NF-y soil (>1) suggesting a weak crystallinity of extractable Fe. Conversely, other soils had Fe_o/Fe_d ratio < 0.5 regardless different deposition age and land use. The significant portion of Fe_o in NF-y, particularly in subsoils (52 g kg^{-1}) was also reflected from the high amount of hydroxylamine hydrochloride extractable iron ($Fe_h = 51$ g kg^{-1}). In NF-y, the SOC percentage bound to Fe (OC_h) was estimated around 34 – 63% whereas it ranged from 14 to 32 % in the other soils.

3.4. Soil classification

According to morphological, physical, and chemical soil properties, most soils fitted the criteria of Andic properties, such as having $Al_o + 1/2Fe_o > 2\%$, bulk density ≤ 0.9 kg dm^{-3}, and phosphate retention ≥ 85% with a combined thickness ≥ 30 cm. The NF-y soils have vitric as well as andic properties since these soils had $Al_o + 1/2Fe_o < 2\%$ and P-retention < 85% in topsoils but fulfill the requirement of andic properties in subsoil. From base saturation, all forest soils receive the qualifier “Dystric”, whereas cultivated soils are “Eutric and Aric”. Full classification names (IUSS, 2015) are in Supplementary information Table 1.

3.5. Total elemental analysis, degree of weathering, and estimation of acid neutralizing capacity

The NF-y soil horizons were clearly set apart with the highest SiO_2 (435 – 699 g kg^{-1}) and SiO_2/R_2O_3 molar ratio ranging from 4.7 to 8.6 (Table 3). In contrast, this ratio was invariably below 2 in all other soils, in which SiO_2 content ranged from 177 to 361 g kg^{-1}. SiO_2 content was inversely proportional to Al_2O_3, and Fe_2O_3 contents. Notable concentrations of Al_2O_3 and Fe_2O_3 were measured in soil horizons under pine forest and crops with no significant differences between these land uses. All studied soils generally had low total contents of CaO, MgO, K_2O,

Table 2
Selected physicochemical properties in surface and sub-surface horizon of studied soils.

Depth	pH		BD	O.C	Particle-size distribution			Exchangeable cations					CEC_T	BS	P-ret.	Oxalate			Fe_d	Fe_o/Fe_d	Fe_h	Al_p	Al_p/Al_o	OC_h	Allo +imo[a]	Volc. glass
	H_2O	KCl			Sand	Silt	Clay	Ca	K	Mg	Na	Al				Al_o	Fe_o	Si_o								
(cm)	–	–	g cm^{-3}	g kg^{-1}	%			$cmol_{(+)}$ kg^{-1}						%	%		g kg^{-1} soil							% of SOC	%	%
Primary forest (NF-y)																										
0–20 (A)	4.08	3.86	0.77	37.1	42.8	38.5	18.7	0.22	0.03	0.06	0.05	3.64	10.1	4	68.5	3.51	15.50	0.06	7.70	2.01	13.33	3.43	0.98	33.99	0.04	4.5
20–40 (AB)	4.39	3.94	0.78	26.0	40	40.18	19.81	0.13	0.03	0.05	0.04	2.04	7.48	4	71.3	2.34	25.42	0.04	16.92	1.50	23.93	3.52	1.50	34.05	0.03	2.3
60–80 (Bw)	4.26	4.00	0.65	28.6	29.2	41.28	29.51	0.13	0.01	0.04	0.03	2.06	7.94	3	85.9	4.83	52.43	0.13	42.58	1.23	51.30	2.81	0.58	62.58	0.09	5.4
Agricultural land (AG-y)																										
0–20 (Ap1)	5.09	4.36	0.67	2.99	8.2	23.58	68.21	7.67	1.29	1.19	0.72	1.08	7.96	137	83.5	14.35	21.08	0.85	42.51	0.50	22.74	26.30	1.83	15.81	0.61	1.3
20–40 (Ap2)	4.97	4.39	0.66	13.0	3.1	33.84	63.06	5.67	0.12	0.84	1.13	0.75	5.64	137	85.6	16.52	12.95	1.42	36.56	0.35	13.10	19.71	1.19	21.59	1.01	1.8
60–80 (Bw)	4.80	4.26	0.64	11.2	5.7	32.87	61.43	4.71	0.21	0.64	0.71	1.24	6.21	101	87.9	22.34	18.13	2.26	57.37	0.32	13.64	12.94	0.58	19.51	1.61	1.7
Pine forest (PF-i)																										
0–20 (A1)	4.54	3.65	0.64	23.6	8	24.73	67.27	1.77	0.08	0.59	0.24	4.79	10.7	25	84.9	8.11	11.89	0.45	33.23	0.36	13.44	41.00	5.06	17.47	0.32	1.9
20–40 (A2)	4.40	3.69	0.61	13.0	6.1	28.44	71.56	0.49	0.05	0.16	0.25	5.59	10.5	9	85.6	10.36	12.15	0.79	40.72	0.30	14.95	32.23	2.97	21.32	0.56	1.9
70–90 (Bw)	4.44	3.60	0.69	5.9	6.4	29.25	64.35	0.22	0.08	0.06	0.38	5.17	10.1	7	87.4	13.73	21.11	1.36	46.13	0.46	19.74	13.70	1.00	31.45	0.97	0.9
Agricultural land (AG-i)																										
0–20 (Ap1)	5.40	4.65	0.66	54.4	25.0	47.77	27.24	6.61	0.62	0.93	0.13	0.59	7.44	111	77.8	31.40	12.28	2.37	31.30	0.39	14.16	7.60	0.24	21.38	1.68	1.1
20–40 (Ap2)	5.75	5.32	0.47	42.6	12.1	52.29	35.62	9.97	0.95	1.75	0.14	0.04	6.00	219	88.1	33.24	12.08	2.66	35.16	0.34	14.81	5.81	0.17	14.17	1.89	1.6
50–70 (Bw)	5.91	5.50	0.52	26.9	12.5	40.44	47.07	6.99	0.63	1.46	0.17	0.03	5.44	172	90.7	36.40	11.57	3.01	29.47	0.39	15.79	5.07	0.14	22.05	2.14	0.1
Pine forest (PF-o)																										
0–20 (A1)	4.73	4.57	0.50	33.3	9.5	35.03	55.48	0.74	0.07	0.15	0.06	1.55	6.98	14	91.0	28.45	17.54	2.19	38.42	0.46	22.89	10.12	0.36	29.41	1.55	0.9
20–40 (A2)	4.88	4.68	0.56	18.2	10.7	42.88	46.63	0.39	0.03	0.11	0.09	1.48	6.43	10	89.3	27.73	17.19	2.22	41.18	0.42	25.88	9.75	0.35	31.60	1.57	1.6
60–80 (AB)	4.42	4.38	0.60	15.7	10.8	40.38	48.82	0.35	0.03	0.16	0.12	2.30	7.25	9	88.3	25.92	17.51	1.04	39.10	0.45	35.06	9.39	0.36	26.62	0.74	0.9
Agricultural land (AG-o)																										
0–20 (Ap1)	5.38	4.52	0.65	47.0	14.5	30.59	54.91	10.45	1.55	1.64	0.14	0.30	9.15	151	86.6	17.07	9.68	1.04	28.14	0.34	14.20	9.00	0.53	15.17	0.74	2.0
20–40 (Ap2)	5.60	4.68	0.61	28.8	12.7	37.27	50.02	6.97	1.62	1.25	0.18	0.10	7.98	126	84.6	15.59	9.46	1.15	28.28	0.33	14.32	8.56	0.55	18.87	0.81	1.9
60–80 (Bw)	5.77	4.73	0.62	7.8	4.9	32.29	62.81	5.99	1.79	0.97	0.23	0.07	7.44	121	87.7	9.08	7.96	0.81	31.68	0.25	13.03	10.66	1.17	16.15	0.58	1.3

[a] Allophane and imogolite = Si_o% x 7.1 (Nanzyo et al., 1993).

Table 3
Geochemical characteristics (oxide content, weathering intensity, acid-neutralizing capacity).

Site	Depth	Al_2O_3	SiO_2	TiO_2	CaO	MgO	K_2O	Na_2O	Fe_2O_3	MnO	P_2O_5	LOI	Weathering index SiO_2/R_2O_3	Weathering index (K + Ca)/Ti	Weathering index CIA	Weathering index TRB	Weathering index Fe_d/Fe_t	Percentage non-exch. base pool to TRB	Acid neutralizing capacity (ANC)
		weight %													%	$cmol_{(+)}$ kg^{-1}		%	$cmol_{(+)}$ kg^{-1}
NF-y	0–20 (A)	6.9	59.6	1.4	1.1	0.7	0.7	0.6	4.6	0.0	0.3	24.1	8.6	1.5	66	106.5	0.24	99.7	589.1
	20–40 (AB)	6.3	69.9	1.9	0.8	0.9	0.6	0.3	7.1	0.1	0.3	12.3	8.9	0.9	71	95.8	0.25	99.7	574.2
	60–80 (Bw)	4.8	43.5	1.7	0.8	0.9	0.4	0.3	13.5	0.1	0.3	33.8	4.7	0.9	68	90.9	0.45	99.8	599.9
AG-y	0–20 (Ap1)	23.3	28.7	1.5	0.3	0.5	0.2	0.1	12.7	0.2	0.4	31.4	1.5	0.2	96	38.9	0.48	72.1	1204
	20–40 (Ap2)	22.9	28.7	1.4	0.2	0.4	0.1	0.1	11.3	0.2	0.4	34.0	1.5	0.2	97	33.2	0.46	76.6	1156.
	60–80 (Bw)	22.2	30.3	1.3	0.3	0.6	0.2	0.1	10.4	0.2	0.4	33.5	1.7	0.3	96	45.6	0.79	86.2	1156.7
PF-i	0–20 (A1)	22.6	36.1	1.4	0.6	0.7	0.2	0.2	11.2	0.2	0.4	25.9	1.9	0.7	93	69.1	0.43	96.1	1076.5
	20–40 (A2)	23.9	30.8	1.6	0.2	0.5	0.1	0.1	13.1	0.2	0.2	28.3	1.5	0.3	97	38.6	0.44	97.5	1212.2
	70–90 (Bw)	24.2	26.5	1.7	0.03	0.5	0.1	0.1	14.2	0.2	0.2	32.0	1.3	0.1	99	30.0	0.46	97.5	1242.3
AG-i	0–20 (Ap1)	21.4	25.1	1.3	1.3	1.2	0.2	0.3	11.7	0.3	1.0	35.4	1.4	1.2	88	118.4	0.39	93.0	1248.5
	20–40 (Ap2)	22.8	18.8	1.3	0.5	0.7	0.2	0.1	11.4	0.2	0.5	42.9	1.0	0.4	95	61.1	0.44	79.0	1295.4
	50–70 (Bw)	22.6	19.5	1.2	0.5	1.2	0.2	0.1	11.1	0.2	0.3	43.1	1.1	0.5	94	84.3	0.38	89.0	1213.3
PF-o	0–20 (A1)	24.8	17.7	1.7	0.1	0.5	0.1	0.1	13.5	0.2	0.4	40.6	0.8	0.1	98	34.7	0.41	97.0	1258.7
	20–40 (A2)	26.4	19.4	1.8	0.2	0.7	0.1	0.1	14.5	0.3	0.4	35.4	0.9	0.2	98	45.2	0.41	98.6	1282.6
	60–80 (AB)	25.4	24.4	1.7	0.1	0.5	0.1	0.1	13.7	0.3	0.3	32.8	1.1	0.1	99	31.1	0.41	97.9	1387.1
AG-o	0–20 (Ap1)	21.3	32.4	1.3	1.1	0.9	0.4	0.3	10.0	0.3	0.8	30.4	1.9	1.1	88	99.1	0.40	86.1	1305.9
	20–40 (Ap2)	21.6	29.7	1.3	0.6	0.7	0.4	0.2	10.8	0.3	0.5	33.6	1.7	0.7	92	71.1	0.38	85.9	1188.9
	60–80 (Bw)	24.8	33.0	1.5	0.2	0.5	0.4	0.1	12.0	0.3	0.3	26.9	1.6	0.3	96	42.7	0.38	79.0	1279.7

Na_2O, with slightly higher levels in NF-y soil horizons. Loss on ignition (LOI) was generally high (12.3 to 43.1%), suggesting that these soils contained substantial amounts of amorphous phases and organic matter.

The weathering indices using ratios of SiO_2/R_2O_3, (K + Ca)/Ti, CIA, and TRB demonstrated the distinctly lower weathering degree of the NF-y soils compared to other soils (Table 3). The NF-y soils had higher SiO_2/R_2O_3 (4.7–8.9), (K + Ca)/Ti (0.9 – 1.5), and lower Fe_d/Fe_t (0.25 – 0.45), and CIA (66 – 71%). In contrast, these weathering indices were low and the CIA was high in other sites indicating more severe weathering close to the ferralitic domain (Herbillon, 1986). TRB was higher in NF-y (91 – 106 $cmol_{(+)}\ kg^{-1}$), AG-i (61 – 118.4 $cmol_{(+)}\ kg^{-1}$), and, but in lesser extent, AG-o (43 – 99 $cmol_{(+)}\ kg^{-1}$), whereas AG-y, PF-i, and PF-o contained TRB ranging from 30 to 60 $cmol_{(+)}\ kg^{-1}$. Our data further showed that, apart from NF-y and AG-y, TRB was always higher in cultivated soils than in their counterparts under pine forest. TRB was negatively correlated ($r = 0.74$) with clay. The percentage of non-exchangeable base pool relative to TRB reached >95% in both primary and pine forest soils, whereas it ranged from 72 to 93% in agricultural soils.

Soil ANC ranged from 574.2 to 1387.1 $cmol_{(+)}\ kg^{-1}$. The NF-y soil clearly had the lowest ANC compared to other soils (574.2 – 600 $cmol_{(+)}\ kg^{-1}$). Apart from NF-y, there were no significant different of ANC between young, intermediate, and old deposition age, but higher ANC was found in pine forest than cultivated soils ($p < 0.05$). Soil ANC was positively correlated to Al_2O_3 and Fe_2O_3 ($r = 0.67$ and $r = 0.68$; $p < 0.01$), respectively.

3.6. XRD-mineralogy

Semi quantitative identification of the mineral phase using XRD revealed the dominance of amorphous materials in most soils (Fig. 3). Amorphous materials in XRD can be defined as all phases that do not produce XRD-peaks (Jones et al., 2000). Their content varied across deposition age and land use. The lowest amorphous content was found in NF-y soils, particularly in the topsoil (±25%). Conversely, other soils contained more amorphous materials with the largest content in the AG-i (±64%). These observations were also supported by high LOI values and a high Al_o + $1/2Fe_o$ content. Estimated contents of amorphous materials were positively correlated with Al_o and Al_o + $1/2Fe_o$ (r ± 0.80, $p < 0.01$), and negatively with SiO_2 ($r = -0.51$, $p < 0.01$) (Fig. 4). There was generally no clear depth gradient in amorphous material content.

As indicated by a broad 0.7-nm peak, 1:1 clay minerals were present in all samples (Fig. 5). The 0.7-nm peak was only weakly expressed (<10%) at NF-y, while in contrast the derived 1:1 clay mineral content was 12% to as much as 34 % in other sites. High contents of this mineral were detected in the topsoil at AG-y and subsoil at AG-o. Minerals from the quartz group, such as quartz, tridymite, and cristobalite/opal were present in notable quantities, especially at NF-y (>30%; sum of the identified minerals). Conversely, the proportion of these minerals ranged only between 7% and 14% at other soils. Other minerals, such as hornblende, andesine, magnetite, gibbsite, albite, and rutile were detected in minor proportions and were not found in all soils. A notable quantity of gibbsite was found at the AG-i and PF-o (8 – 15%), whereas it was found in small amount in NF-y (0.1 – 0.3%). These minerals also showed no clear trend with depth. Grouping the minerals identified by Q-XRD in either primary minerals (Albite, Cristobalite, Trydimite, Quartz, Rutile, Andesine, Alunite and Hornblende) or secondary minerals (Gibbsite, 1:1 minerals; Magnetite and Hematite) showed clearly higher amounts of primary minerals and lower amounts of secondary minerals in NF-y, compared to the other soils.

3.7. Soil specific surface area

Soil SSA and micropores volume did not differ among soils, except for a contrast between NF-y and the other soils (Fig. 6). Natural forest nevertheless did exhibit a low SSA (8 – 58 $m^2\ g^{-1}$) compared to pine forest and cultivated soils (66 – 198 $m^2\ g^{-1}$). The largest surface area was detected in the subsoil of AG-i (198 $m^2\ g^{-1}$), in accordance with high contents of Al_o and amorphous materials. Most of the subsoil had higher SSA than in topsoil. The volume of micropores was between 0 and 19.4 $mm^3\ g^{-1}$ and large micropore volume was detected in AG-y, AG-i,

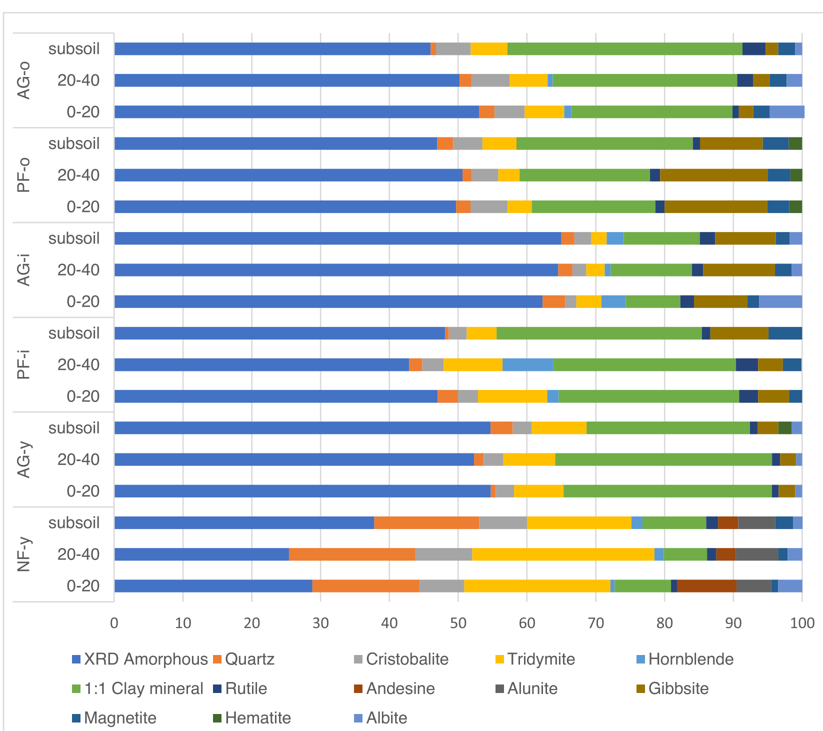

Fig. 3. Relative proportions of mineral constituents as inferred by XRD data in the studied soil.

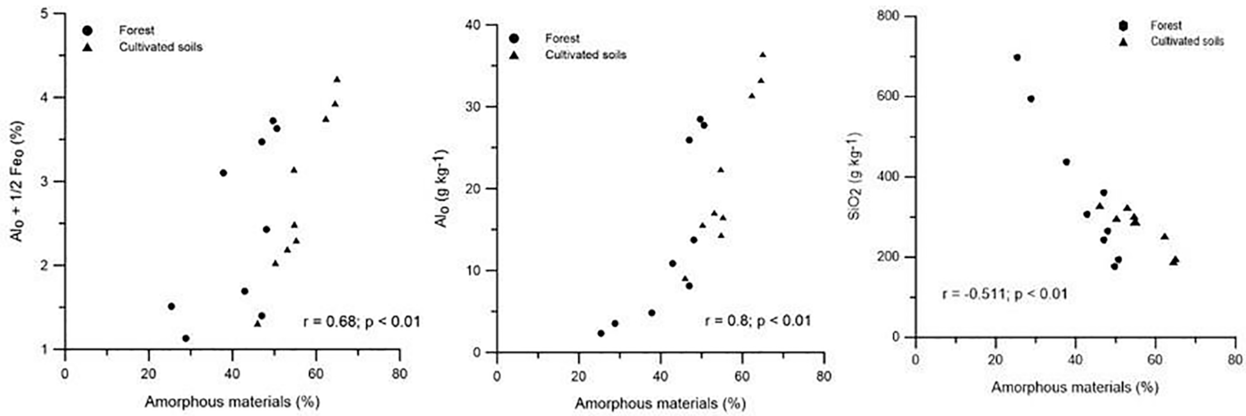

Fig. 4. Correlations between XRD-amorphous materials and content of Al_o, $Al_o + 1/2Fe_o$, and SiO_2.

and PF-o soils. The C_{BET} constant, which relates to the affinity of sorption of N_2 gas molecules on solid surfaces, ranged from 75 to 213 indicating high energy surface sites or the filling of narrow micropores (Thommes et al., 2015). This high value was detected in most of the soils, except NF-y and AG-o. SSA, micropores, and C_{BET} were positively correlated with Al_o ($r > 0.50$; $p < 0.01$) (Fig. 7).

4. Discussion

4.1. *Verifying the anthropo-chronosequence and soil weathering stage as affected by deposition age*

Though soil sampling was based on geological maps and land use data, we verify here whether our analytical results confirm or not that the sequence is an anthropo-chronosequence. Clearly, NF-y is an outlier in its mineralogical composition, having higher amounts of primary minerals with notably higher amounts of Si-rich minerals, and having lower amounts of amorphous material and 1:1 minerals but slightly higher amounts of crystalline Fe-minerals (Fig. 3). Based on the weathering indices and silica oxide contents (Table 3), it is also clear that the NF-y soil is less weathered than all other soils. The high amount of SiO_2 (±60%) and less Al_2O_3 (6%) are characteristic of a more siliceous composition of the ash. A significant portion of SiO_2 content was possibly derived from volcanic glass and other silicate minerals (i.e. tridymite, cristobalite and quartz). The low SSA at NF-y further indicates a limited degree of physical weathering, which is known to lift the surface area of minerals (e.g. quartz < potassium feldspar < anorthite), probably due to the development of internal porosity (Brantley and Mellott, 2000). In addition, the coarser texture (±29 – 40% sand particle), particularly in the topsoil of NF-y also denoted a low weathering intensity. Given the divergent mineralogical composition and total elements in NF-y soil, it is likely that this soil was influenced by the small-scale, more dacitic, eruption of nearby (1.3 km) Mount Tangkuban Perahu in 1910 (Surmayadi et al., 2011), and that the parent material at this site was rejuvenated by younger ash of more siliceous composition. As a conclusion, the NF-y soils is developed from another parent material, thus the chronosequence covers 3 ages of parent materials: mixed old/young (NF-y), near 8700 years (AG-y, PF-i, AG-i), and near 10000 years (PF-o, AG-o). This means that NF–y should be kept out of the comparison between different land uses because NF-y and AG-y are in different parent materials.

Apart from the different weathering intensity of NF-y soils, all the weathering indices including ratios of SiO_2/R_2O_3, $(K + Ca)/Ti$, Fe_d/Fe_t, CIA, and TRB showed that the studied soils had no significant difference based on deposition age (i.e. intermediate and old deposition age). The proportion of various identified minerals in the study soils, except NF-y, were also comparable. Solleiro-Rebolledo et al. (2015) suggested that the Andosol stage remains stable as long as the parent materials still contain sufficient materials to form allophane. Indeed, we found that volcanic glass was not exhausted at any of the studied soils (Table 2). The limited contrast in weathering between young, intermediate, and old deposition ages of pine forest and cultivated soils may be due to the relatively small deposition age differences: i.e. possibly from the Holocene to Late Pleistocene, ± 8000 – 10,000 yrs old (Table 1).

4.2. *Effects of land use on weathering and acid-neutralizing capacities*

Cultivated soils were detected to have higher $(K + Ca)/Ti$ ratio, TRB, and lower CIA than pine forest soils ($p < 0.01$) indicating lower weathering intensity in cultivated soils than pine forest. Another weathering index, ratio Fe_d/Fe_t, which is independent from the total content of Si, Al, Ca, Mg, Na, K showed no significant difference between soils in these land use. These results highlighted the contribution of cropland management on the total base cations.

The TRB followed a sequence AG-y < PF-o < PF-i < AG-o < AG-i < NF-y indicating that the most and least weathered soil was found in AG-y and NF-y, respectively. All soils generally have reached an advanced weathering stage since fresh andesitic materials can have TRB values as high as 500 $cmol_{(+)}\ kg^{-1}$, with some being close to ferralitic domain as computed at ≤ 40 – 60 $cmol_{(+)}\ kg^{-1}$ (e.g. PF soil) (Herbillon, 1986) (Fig. 8). High rainfall was possibly one of the reasons of advanced weathering stage, similar to the recent study by Vander Linden et al. (2021). Higher weathering degrees of pine forests soils based on the low TRB possibly links to the effect of deforestation. Clear-cutting was observed to increase export of base cations from forest soils (Richardson et al., 2017). In addition, the acidic condition in pine forest soils (pH_{H2O} 4.4 – 4.7) results in the decrease of base cations and increase of acid cations. On the other hand, different weathering levels on cultivated soils likely occur because not all croplands have been equally managed in term of the intensities of tillage, fertilization, and type of crops, thus the cultivation age alone is not the sole determinant of weathering stage.

The ability of soil to neutralize net acidification (ANC) is commonly linked to the released of alkaline cations through mineral weathering. Since the major component of ANC is TRB, we expected a high ANC in cultivated soils. Interestingly, higher ANC was detected in pine forest soils than cultivated soils ($p < 0.01$). A decrease of ANC is linked to net acidification of soil (Van Breemen et al., 1983) which causes a significant leaching of Fe, Al, and Mn (Nawaz et al., 2013). However, our study showed no significant correlation between ANC and pH, and higher Al_2O_3 and Fe_2O_3 contents in pine forest than cultivated soils ($p < 0.01$). This result was also concomitant with the similar amount of base cations in the non-exchangeable pool between those soils. The fact that pine forest soil had more Al_2O_3 and Fe_2O_3, and similar amount of non-exchangeable base cations suggested that not all minerals weathered faster at low pH in these soils.

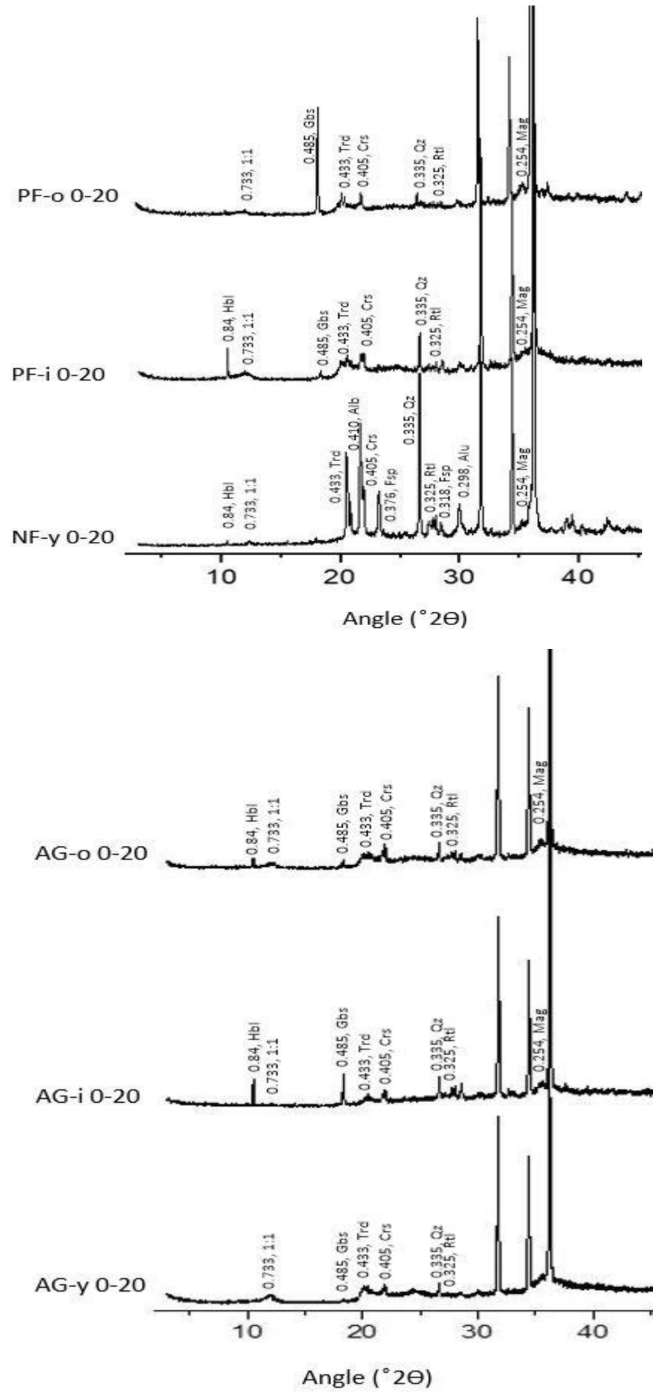

Fig. 5. Powder Diffractogram of soil samples (<2 mm) at depth 0–20 in forest (top) and agricultural (bottom) sites. Peak d-spacings are indicated in nm. Mineral abbreviations: 1:1: 1:1 clay minerals, Hbl: hornblende, Trd: tridymite, Alb: albite, Crs: cristobalite, Gbs: gibbsite, Fsp: feldspar, Qz: quartz, Rtl: rutile, Alu: alunite, Mag: magnetite.

4.3. Effects of land use on soil properties

Several soil properties were clearly distinct in cultivated soil compared to forests (i.e. excluding NF-y). Cultivated soils had a generally higher pH, OC stock, exchangeable bases, base saturation, and P_2O_5 level ($p < 0.05$) than the forests (Table 4). The higher P levels logically derive from substantial annual inputs of fertilizers and manure (Table 1). Likewise, lime and manure application explain the higher pH and so the exchangeable bases and TRB, particularly Ca, of the cultivated soils. Higher OC stock was detected in cultivated soils, in line with the recent study by Ouédraogo et al. (2020). Conversely, continuous nutrient loss through leaching with insufficient replenishment by weathering likely acidified the forest soils with consequent lower base saturation. Similar effects of agricultural practices on soil properties were also found by Anda and Dahlgren (2020), who recently compared cropland and forest soils in the same region. Other properties that were expected to be equally sensitive to agricultural practices (i.e. master properties) (Kuzyakov and Zamanian, 2019) such as bulk density, surprisingly did not differ between forest and cultivated soils. Anda and Dahlgren (2020) did find a somewhat lower bulk density in pine forest (0.4 g cm^{-3}) than in cultivated soils (0.5 – 0.8 g cm^{-3}) but regardless both studies show that bulk density is inherently very low in these soils, as expected for Andosols, with little further effect of land-use. Shoji and Takahashi (2002) also confirmed that a low bulk density remains in Andosols even after long-term cultivation.

Other than the land-use effects described above, the content of non– to poorly-crystalline-Al in cultivated soils was 14% higher than in pine forest, but with limited replication this difference could not be statistically demonstrated. Nevertheless, this outcome is well in line with a study of Andosols on the Galápagos by Gerzabek et al. (2019) who likewise documented Al_o in cropland topsoils to be 9% higher when compared to directly adjacent forest from which the agricultural land was developed. Formation of aluminum oxides as a result of agricultural practices in volcanic soils was reported by Hernández et al. (2012) as well. Firstly, long term organic amendments were reported to increase amorphous Al and pH (Yu et al., 2017; Zhang et al., 2017). These organic amendments would promote the formation of short-range order minerals possibly due to production of low molecular weight organic acids by roots or the degradation of organic amendments (Yu et al., 2017). Secondly, deforestation and soil tillage possibly cause an increase of soil temperature (Shen et al., 2018), enhancing chemical weathering (Li et al., 2021).

Our study then showed that within similar soil genoforms, a soil phenoform developed over agricultural periods in<50 years. These phenoforms are expressed in the soil classification by either the WRB-qualifier *dystric* (forest soils) or *eutric* (agricultural soils). In the agricultural soils, the qualifier *aric* was assigned, but not in forest soils. At the level of soil variables, the soil phenoforms were expressed by a difference in attributes such as pH, exchangeable cations, base saturation, OC stock, and major elements (MnO and P_2O_5). The change of these attributes will possibly affect nutrient cycling. Generally, agriculture practices will alter the "master properties" to reach their maximum or minimum with time, but the rate of alteration is still under discussion (Kuzyakov and Zamanian, 2019).

4.4. Soil organic carbon and its association with minerals

The total OC stocks at topsoil (0–40 cm) and subsoil (±60-80 cm) varied in the order of (kg m^{-2}): AG-i (13.9) > NF-y (13.7) > AG-o (10.6) > AG-y (7.2) ~ PF-o (7.2) > PF-i (5.4). Pine forest soils thus generally had lower SOC stocks than agricultural and primary forest soils, in accordance with other studies (Anda and Dahlgren, 2020; La Manna et al., 2018). The particularly low SOC stocks in pine forest were unexpected because usually the more polyphenol and lipid-rich residues from coniferous species give rise to accumulation of OM in soil, owing to their inherent low decomposability (McTiernan et al., 2003). The resulting ectorganic layers can in turn further limit accumulation of SOC in the underlying mineral soil because then plant litter is not completely incorporated. In any case it is striking that there was apparently no OC depletion after conversion from forest to agricultural land-use as otherwise generally expected (Murty et al., 2002; Don et al., 2011). It seems improbable that the inputs of OC via manure and vegetable crops residues would have sufficed to explain the absence of a contrast in OC content with the pine forest soils. In fact, the OC content at AG-y was substantially lower than at AG-i and AG-o, although at the former site

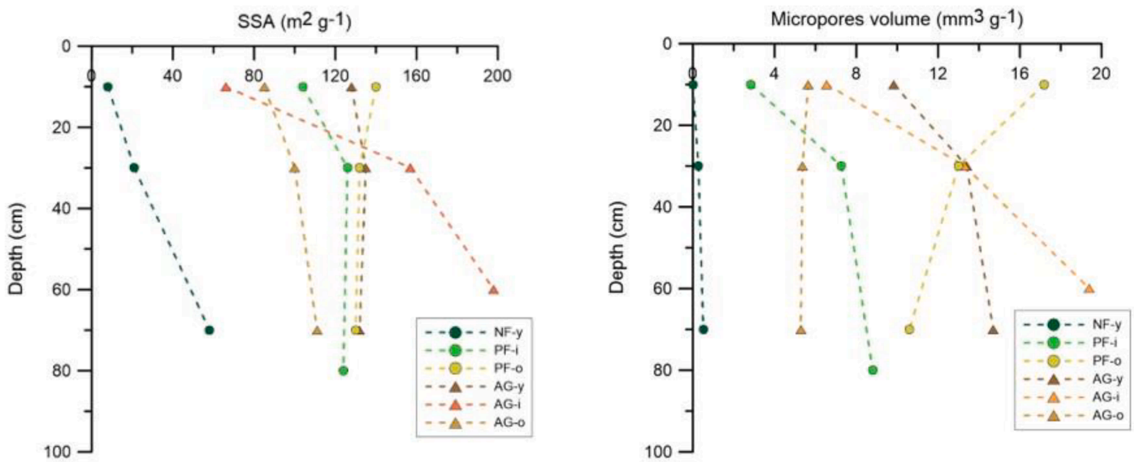

Fig. 6. Depth evolution soil specific surface area (left) and micropores volume (right) in the different soils at each site.

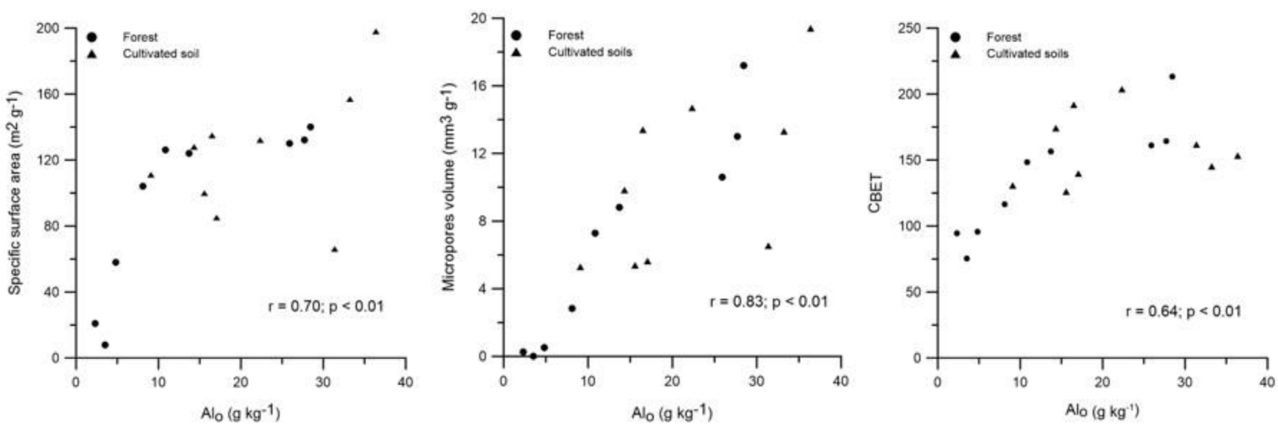

Fig. 7. Specific surface area, micropores volume, and C_{BET} as plotted against Al_o content in soils.

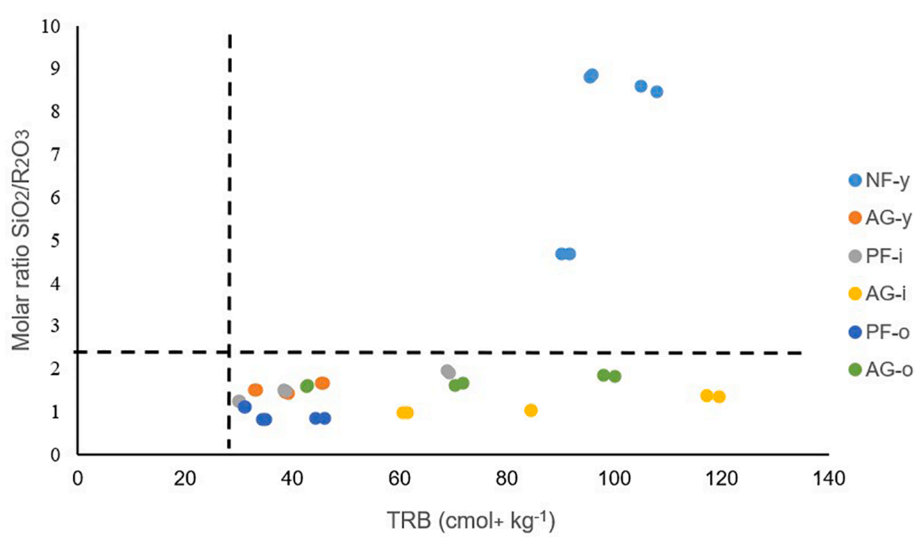

Fig. 8. Plot of molar ratio SiO_2/R_2O_3 versus TRB in soils at each site.

huge amounts of organic and NPK fertilizers (±76 and 2 Mg ha^{-1} y^{-1}, respectively) are being applied. The SOC content is obviously the resultant of the balancing of both OC inputs as well as outputs, of which microbially mediated decomposition is by far most important. Various mechanisms simultaneously limit OM decomposition in soil, of which sorption onto reactive minerals and metals has been long recognized for volcanic soils. More specifically, direct ligand exchange between organic functional groups and hydroxylated surfaces on short-range ordered mineral phases and the formation of organo-metal complexes have been shown to be very effective carbon retention mechanisms in volcanic soils

Table 4
Comparison of mean soil properties in the forest and agricultural sites (independent samples *t*-test).

Soil properties	Unit	Forests	Agriculture	p-value
pH_{H2O}	–	4.57 ± 0.19	5.41 ± 0.38	0.001
Exchangeable Ca	$cmol_{(+)}\ kg^{-1}$	0.66 ± 0.54	7.23 ± 1.85	0.001
Exchangeable Mg	$cmol_{(+)}\ kg^{-1}$	0.20 ± 0.18	1.18 ± 0.37	0.001
Exchangeable K	$cmol_{(+)}\ kg^{-1}$	0.06 ± 0.02	0.98 ± 0.60	0.001
Exchangeable Na	$cmol_{(+)}\ kg^{-1}$	0.19 ± 0.12	0.40 ± 0.36	0.161
Exchangeable Al	$cmol_{(+)}\ kg^{-1}$	3.48 ± 1.82	0.47 ± 0.46	0.001
CEC_T	$cmol_{(+)}\ kg^{-1}$	8.66 ± 1.90	7.03 ± 1.30	0.034
Organic carbon stock	$ton\ ha^{-1}$	22.56 ± 7.52	38.71 ± 19.03	0.017
Base saturation	%	12.51 ± 6.82	142 ± 38.58	0.001
Al_o	$g\ kg^{-1}$	19.13 ± 8.85	21.78 ± 9.37	0.236
$Al_o + 1/2Fe_o$	%	2.24 ± 0.84	2.60 ± 0.91	0.175
P_2O_5	%	0.30 ± 0.11	0.49 ± 0.22	0.006
Amorphous materials	%	47.57 ± 2.71	55.78 ± 6.80	0.034

(Basile-Doelsch et al., 2015, 2005; Kleber et al., 2015; Lehmann and Kleber, 2015; Sanderman and Kramer, 2017; Tamrat et al., 2019).

In pine forest and cultivated soils, Al_o correlated positively with OC content across the different sampled depths (Fig. 9). This suggests that, as reported by previous studies (Hernández et al., 2012; Ouédraogo et al., 2020), association by non-crystalline materials was likely a significant OC stabilization mechanism. Al_o content also correlated well with SSA, C_{BET}, and even a bit stronger with micropores volume. Soils with high microporosity generally have high C_{BET} (Mayer and Xing, 2001; Wagai et al., 2009), thus clearly a substantial share of colloidal surface was provided by pedogenic Al. The limited microbial accessibility of OM held in micropores on pedogenic oxides has been particularly forwarded to raise long-term stability of mineral-retained OM (Zimmerman et al., 2004). So, we hypothesize that the larger surface and micropore volume provided by the higher Al_o under cultivated soils in part explains their elevated OC content compared to pine forest soil. A likewise promoted formation of Fe_o by land-use conversion was not observed and the here estimated pedogenic Fe-bound C levels remained comparable between pine forest and cultivated soils. The interaction between non-crystalline Al and OC was furthermore probably stronger in subsoils ($R^2 = 0.88$; $p < 0.01$) than in the 0–40 cm topsoil ($R^2 = 0.30$; $p < 0.01$) (Fig. 9). Probably, at the lower SOC concentrations found in the subsoils (Fig. 9), more reactive mineral surface could be occupied by the OM, while high OM levels in topsoil may have overloaded the available reactive mineral surface, as also suggested by Gulde et al. (2008). Di et al. (2017) also found that in Chinese cropland soils with high manure inputs, the potential to store additional SOC declined, which these authors attributed to a lower SOC saturation deficit.

5. Conclusions and research perspective

Apart from one rejuvenated volcanic ash soil, the anthropo-chronosequence in our study had comparable ages and parent materials, and thus are suitable to determine the effect of human land use. The data presented in this study clearly indicate the increase of base cations retention due to the decrease of acidification as natural forest is converted into managed ecosystems. Under agricultural practices (30 – 50 years), chemical soil properties such as pH, OC stocks, exchangeable cations, and base saturation were changed and can be considered to be an expression of soil phenoforms. Strikingly, we found an increase of OC stock and no change in bulk density under cultivated soils. We hypothesize that the higher observed SRO aluminum, SSA, and micropores volume under anthropogenic sites (i.e. pine forest and agriculture) promoted retention of SOC, particularly in the subsoil. The relation between minerals and OC may be better clarified by taking into account (i) the rate of mineral weathering, (ii) the capacity of soils to absorb OC relative to the OC-input via agricultural practices, and (iii) the OM

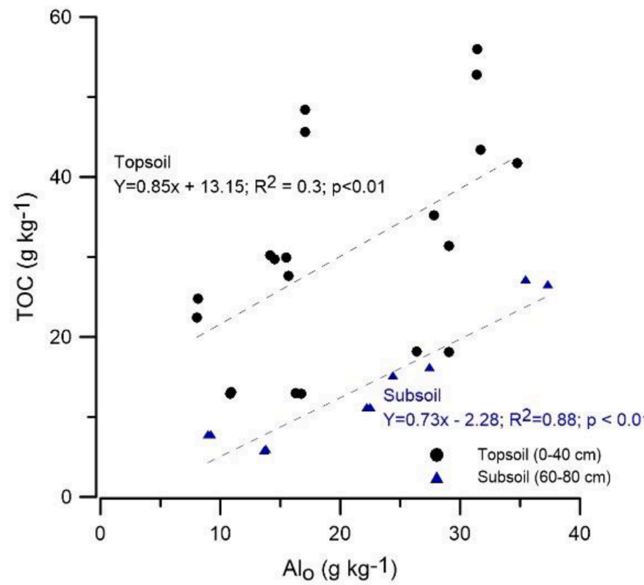

Fig. 9. Relation between SOC and Al_o content in topsoil (0 – 40 cm) and subsoil of pine forest and cultivated soils.

turnover as function of mineralogical properties.

Declaration of Competing Interest

The authors declare that they have no known competing financial interests or personal relationships that could have appeared to influence the work reported in this paper.

Acknowledgement

This work was funded and supported by Indonesia Endowment Fund for Education (LPDP; Grant number 201801220212290). The XRD facilities were subsidized by the Hercules Foundation and the Research Foundation – Flanders (FWO-Vlaanderen) through grant numbers AUGE/13/05 – G0F2714N and G028714N. We thank the anonymous reviewers for their valuable comments and suggestions.

Appendix A. Supplementary data

Supplementary data to this article can be found online at https://doi.org/10.1016/j.geoderma.2022.115963.

References

Anda, M., Dahlgren, R.A., 2020. Long-term response of tropical Andisol properties to conversion from rainforest to agriculture. Catena 194, 104679. https://doi.org/10.1016/j.catena.2020.104679.

Anderson, J.U., 1961. An Improved Pretreatment for Mineralogical Analysis of Samples Containing Organic Matter1. Clays Clay Miner. 10, 380–388. https://doi.org/10.1346/ccmn.1961.0100134.

Arifin, M., 1994. Pedogenesis andisol berbahan induk abu volkan andesit dan basalt pada beberapa zona agroklimat di daerah perkebunan teh Jawa Barat. Institut Pertanian Bogor. http://repository.ipb.ac.id/handle/123456789/2518.

Asio, V.B., Jahn, R., Stahr, K., 1999. Changes in the properties of a volcanic soil (Andisol) in Leyte due to conversion of forest to other land uses. Philipp. J. Sci. 128, 1–13.

Balai Besar Litbang Sumberdaya Lahan Pertanian (BBSDLP), 2017. ATLAS PETA TANAH SEMI DETAIL Skala 1:50.000 Kabupaten Bandung Barat Provinsi Jawa Barat. Balai Besar Litbang Sumberdaya Lahan Pertanian, Bogor.

Bandyopadhyay, K.K., 2019. Effect of tillage on soil carbon sequestration. In: Ghosh, P., Mahanta, S., Mandal, D., Mandal, B., Ramakrishnan, S. (Eds.), Carbon Management in Tropical and Sub-Tropical Terrestrial Systems. Springer, Singapore, pp. 213–229. https://doi.org/10.1007/978-981-13-9628-1_13.

Bartoli, F., Burtin, G., Herbillon, A.J., 1991. Disaggregation and clay dispersion of Oxisols: Na resin, a recommended methodology. Geoderma 49, 301–317. https://doi.org/10.1016/0016-7061(91)90082-5.

Basile-Doelsch, I., Amundson, R., Stone, W.E.E., Masiello, C.A., Bottero, J.Y., Colin, F., Masin, F., Borschneck, D., Meunier, J.D., 2005. Mineralogical control of organic carbon dynamics in a volcanic ash soil on La Réunion. Eur. J. Soil Sci. 56, 689–703. https://doi.org/10.1111/j.1365-2389.2005.00703.x.
Basile-Doelsch, I., Balesdent, J., Rose, J., 2015. Are interactions between organic compounds and nanoscale weathering minerals the key drivers of carbon storage in soils? Environ. Sci. Technol. 49, 3997–3998. https://doi.org/10.1021/acs.est.5b00650.
Bergmann, J., Fridel, P., Kleeberg, R., 1998. BGMN- a new fundamental parameter based Rietveld program for laboratory X-ray sources, its use in quantitative analysis and structure investigations. CPD Newsletter, Comm. Powder Diffraction. Int. Union Crystallogr. 20, 5–8.
Birkeland, P.W., 1999. Soils and Geomorphology, 3rd ed. Oxford University Press, New York.
Blake, G.R., Hartge, K.H., 1986. Bulk density, in: Klute, A. (Ed.), Methods of Soil Analysis, Part I. Physical and Mineralogical Methods. ASA SSSA, Madison, WI, pp. 74–75. https://doi.org/10.2136/sssabookser5.1.2ed.c13.
Blakemore, L., Searle, P., Daly, B., 1981. Methods for chemical analysis of soils. https://doi.org/10.1111/aos.12317.
Brahy, V., Deckers, J., Delvaux, B., 2000. Estimation of soil weathering stage and acid neutralizing capacity in a toposequence Luvisol-Cambisol on loess under deciduous forest in Belgium. Eur. J. Soil Sci. 51, 1–13. https://doi.org/10.1046/j.1365-2389.2000.00285.x.
Brantley, S.L., Mellott, N.P., 2000. Surface Area and Porosity of Silicates. Am. Mineral. 85, 1767–1783.
Chadwick, O.A., Gavenda, R.T., Kelly, E.F., Ziegler, K., Olson, C.G., Crawford Elliott, W., Hendricks, D.M., 2003. The impact of climate on the biogeochemical functioning of volcanic soils. Chem. Geol. 202, 195–223. https://doi.org/10.1016/j.chemgeo.2002.09.001.
Chartres, C., Van Reuler, H., 1985. Mineralogical changes with depth in a layered Andosol near Bandung, Java (Indonesia). J. Soil Sci. 1985 (36), 173–186.
Dam, M.A.C., Suparan, P., Nossin, J.J., Voskuil, R.P.G.A., 1996. A chronology for geomorphological developments in the greater Bandung area. West-Java, Indonesia, Journal of Southeast Asian Earth Sciences. 14 (1-2), 101–115.
Delvaux, B., Herbillon, A.J., Vielvoye, L., 1989. Characterization of a weathering sequence of soils derived from volcanic ash in Cameroon. Taxonomic, mineralogical and agronomic implications. Geoderma 45, 375–388. https://doi.org/10.1016/0016-7061(89)90017-7.
Di, J., Feng, W., Zhang, W., Cai, A., Xu, M., 2017. Soil organic carbon saturation deficit under primary agricultural managements across major croplands in China. Ecosyst. Heal. Sustain. 3 (7), 1364047.
Doebelin, N., Kleeberg, R., 2015. Profex: A graphical user interface for the Rietveld refinement program BGMN. J. Appl. Crystallogr. 48, 1573–1580. https://doi.org/10.1107/S1600576715014685.
Don, AXEL, Schumacher, JENS, Freibauer, ANNETTE, 2011. Impact of tropical land-use change on soil organic carbon stocks - a meta-analysis. Glob. Chang. Biol. 17 (4), 1658–1670.
Droogers, P., Bouma, J., 1997. Soil Survey Input in Exploratory Modeling of Sustainable Soil Management Practices. Soil Sci. Soc. Am. J. 61, 1704–1710. https://doi.org/10.2136/sssaj1997.03615995006100060023x.
Gerzabek, M.H., Bajraktarevic, A., Keiblinger, K., Mentler, A., Rechberger, M., Tintner, J., Wriessnig, K., Gartner, M., Valenzuela, X.S., Troya, A., Couenberg, P.M., Jäger, H., Carrión, J.E., Zehetner, F., 2019. Agriculture changes soil properties on the Galápagos Islands-two case studies. Soil Res. 57, 201–214. https://doi.org/10.1071/SR18331.
Gillman, G.P., Sumpter, E.A., 1986. Modification to the compulsive exchange method for measuring exchange characteristics of soils. Aust. J. Soil Res. 24, 61–66. https://doi.org/10.1071/SR9860061.
Gulde, S., Chung, H., Amelung, W., Chang, C., Six, J., 2008. Soil Carbon Saturation Controls Labile and Stable Carbon Pool Dynamics. Soil Sci. Soc. Am. J. 72, 605–612. https://doi.org/10.2136/sssaj2007.0251.
Harrington, C.D., Whitney, J.W., 1987. Scanning electron microscope method for rock-varnish dating. Geology 15, 967–970. https://doi.org/10.1130/0091-7613(1987)15.
Herbillon, 1986. Chemical estimation of weatherable minerals present in the diagnostic horizons of low activity clay soils. In: Beinroth, F., Camargo, M., Eswaran, H. (Eds.), Proceedings of the 8th International Clay Classification Workshop: Classification, Characterization and Utilization of Oxisols (Part 1). Rio de Janeiro, pp. 39–48.
Hernández, Z., Almendros, G., Carral, P., Álvarez, A., Knicker, H., Pérez-Trujillo, J.P., 2012. Influence of non-crystalline minerals in the total amount, resilience and molecular composition of the organic matter in volcanic ash soils (Tenerife Island, Spain). Eur. J. Soil Sci. 63, 603–615. https://doi.org/10.1111/j.1365-2389.2012.01497.x.
IUSS, 2015. World Reference Base for Soil Resources 2014, update 2015 International soil classification system for naming soils and creating legends for soil map, World Soil Resources Reports No. 106. Rome. https://doi.org/10.1017/S0014479706394902.
Jones, R.C., Babcock, C.J., Knowlton, W.B., 2000. Estimation of the Total Amorphous Content of Hawai'i Soils by the Rietveld Method. Soil Sci. Soc. Am. J. 64, 1100–1108. https://doi.org/10.2136/sssaj2000.6431100x.
Kartadinata, M., Okuno, M., Nakamura, T., Kobayashi, T., 2002. Eruptive history of Tangkuban Perahu Volcano, West Java, Indonesia: A preliminary report. J. Geog. 111, 404–409. https://doi.org/10.1017/cbo9781316155530.002.
Kleber, M., Eusterhues, K., Keiluweit, M., Mikutta, C., Mikutta, R., Nico, P.S., 2015. Mineral-Organic Associations: Formation, Properties, and Relevance in Soil Environments. In: Sparks, D. (Ed.), Advances in Agronomy. Elsevier Ltd, pp. 1–140. https://doi.org/10.1016/bs.agron.2014.10.005.
Kuzyakov, Y., Zamanian, K., 2019. Reviews and syntheses: Agropedogenesis-Humankind as the sixth soil-forming factor and attractors of agricultural soil degradation. Biogeosciences 16, 4783–4803. https://doi.org/10.5194/bg-16-4783-2019.
La Manna, L., Gaspar, L., Rostagno, C.M., Quijano, L., Navas, A., 2018. Soil changes associated with land use in volcanic soils of Patagonia developed on dynamic landscapes. Catena 166, 229–239. https://doi.org/10.1016/j.catena.2018.03.025.
Lehmann, J., Kleber, M., 2015. The contentious nature of soil organic matter. Nature 528, 60–68. https://doi.org/10.1038/nature16069.
Lemenih, M., Karltun, E., Olsson, M., 2005. Assessing soil chemical and physical property responses to deforestation and subsequent cultivation in smallholders farming system in Ethiopia. Agric. Ecosyst. Environ. 105, 373–386. https://doi.org/10.1016/j.agee.2004.01.046.
Li, J., Du, J., Zhong, S., Ci, E., Wei, C., 2021. Changes in the profile properties and chemical weathering characteristics of cultivated soils affected by anthropic activities. Sci. Rep. 11, 20822. https://doi.org/10.1038/s41598-021-00302-w.
Maillard, É., Angers, D.A., 2014. Animal manure application and soil organic carbon stocks: A meta-analysis. Glob. Chang. Biol. 20, 666–679. https://doi.org/10.1111/gcb.12438.
Mayer, L.M., Xing, B., 2001. Organic Matter-Surface Area Relationships in Acid Soils. Soil Sci. Soc. Am. J. 65, 250–258. https://doi.org/10.2136/sssaj2001.651250x.
McKeague, J.A., 1967. An evaluation of 0.1 M pyrophosphate and pyrophosphate-dithionite in comparison with oxalate as extractants of the accumulation products in podzols and some other soils. Can. J. Soil Sci. 47, 95–99. https://doi.org/10.4141/cjss67-017.
McTiernan, K.B., Coûteaux, M.M., Berg, B., Berg, M.P., De Anta, R.C., Gallardo, A., Kratz, W., Piussi, P., Remacle, J., De Santo, A.V., 2003. Changes in chemical composition of Pinus sylvestris needle litter during decomposition along a European coniferous forest climatic transect. Soil Biol. Biochem. 35, 801–812. https://doi.org/10.1016/S0038-0717(03)00107-X.
Mehra, O.P., Jackson, M.L., 1958. Iron Oxide Removal from Soils and Clays by a Dithionite-Citrate System Buffered with Sodium Bicarbonate. Clays Clay Miner. 7, 317–327. https://doi.org/10.1346/ccmn.1958.0070122.
Murty, D., Kirschbaum, M.U.F., McMurtrie, R.E., McGilvray, H., 2002. Does conversion of forest to agricultural land change soil carbon and nitrogen? a review of the literature. Glob. Chang. Biol. 8, 105–123. https://doi.org/10.1046/j.1354-1013.2001.00459.x.
Nanzyo, M., Dahlgren, R., Shoji, S., 1993. Chemical Characteristics of Volcanic Ash Soils. In: Shoji, S., Nanzyo, M., Dahlgren, R. (Eds.), Volcanic Ash Soils. Genesis, Properties and Utilization. Elsevier, Tokyo, Japan, pp. 145–187. https://doi.org/10.1016/S0166-2481(08)70267-8.
Nawaz, R., Parkpian, P., Arshad, M., Ahmad, F., Garivait, H., Ali, A.S., 2013. Mobilization and leaching of trace elements (Fe, Al and Mn) in agricultural soils as affected by simulated acid rain. Asian J. Chem. 25, 9891–9896. https://doi.org/10.14233/ajchem.2013.15560.
Nesbitt, H.W., Young, G.M., 1982. Early proterozoic climates and plate motions inferred from major element chemistry of lutites. Nature 299, 715–717. https://doi.org/10.1038/299715a0.
Ouédraogo, R.A., Chartin, C., Kambiré, F.C., van Wesemael, B., Delvaux, B., Milogo, H., Bielders, C.L., 2020. Short and long-term impact of urban gardening on soil organic carbon fractions in Lixisols (Burkina Faso). Geoderma 362, 114110. https://doi.org/10.1016/j.geoderma.2019.114110.
Parfitt, R.L., Milton, R., Orbell, G.E., 1983. Weathering sequence of soils from volcanic ash involving allophane and halloysite New Zealand. Geoderma 29, 41–57. https://doi.org/10.1016/0016-7061(83)90029-0.
Perhutani, 2014. Rencana pengaturan kelestarian hutan; Jangka perusahaan 1 Januari 2012/31 Desember 2021.
Richardson, J.B., Petrenko, C.L., Friedland, A.J., 2017. Base cations and micronutrients in forest soils along three clear-cut chronosequences in the northeastern United States. Nutr. Cycl. Agroecosystems 109, 161–179. https://doi.org/10.1007/s10705-017-9876-4.
Rossiter, D.G., Bouma, J., 2018. A new look at soil phenoforms – Definition, identification, mapping. Geoderma 314, 113–121. https://doi.org/10.1016/j.geoderma.2017.11.002.
Rouiller, J., Burtin, G., Souchier, B., 1972. La dispersion des sols dans l'analyse granulométrique. Méthode utilisant les résines échangeuses d'ions. Bull. ENSAIA Nancy 194–205.
Sanderman, J., Kramer, M.G., 2017. Dissolved organic matter retention in volcanic soils with contrasting mineralogy: a column sorption experiment. Biogeochemistry 135, 293–306. https://doi.org/10.1007/s10533-017-0374-1.
Shen, Y., McLaughlin, N., Zhang, X., Xu, M., Liang, A., 2018. Effect of tillage and crop residue on soil temperature following planting for a Black soil in Northeast China. Sci. Rep. 8, 1–9. https://doi.org/10.1038/s41598-018-22822-8.
Shoji, S., Dahlgren, R., Nanzyo, M., 1993. Genesis of Volcanic Ash Soils. In: Shoji, S., Nanzyo, M., Dahlgren, R. (Eds.), Volcanic Ash Soils - Genesis, Properties and Utilization. Elsevier Science, pp. 37–71. https://doi.org/10.1016/S0166-2481(08)70264-2.
Shoji, S., Takahashi, T., 2002. Environmental and Agricultural Significance of Volcanic Ash Soils. Glob. J. Environ. Res. 6, 113–135.
Silitonga, P.H., 1973. Peta geologi Lembar Bandung, Djawa (Geologic map of the Bandung Quadrangle. Java), scale 1:100 000.
Sing, K.S., Everett, D., Haul, R.A., Moscou, L., Pierotti, R., Rouquerol, J., Siemieniewska, T., 1985. Reporting physisorption data for gas/solid systems with special reference to the determination of surface area and porosity. Pure Appl. Chem. 57, 603–619.

Solleiro-Rebolledo, E., Sedov, S., Cabadas-Báez, H., 2015. Use of soils and palaeosols on volcanic materials to establish the duration of soil formation at different chronological scales. Quat. Int. 376, 5–18. https://doi.org/10.1016/j.quaint.2014.12.002.

Sosnowska, A., 2012. Land use change impact on soil organic matter. Loess landscape case study. Misc. Geogr. 16, 11–15. https://doi.org/10.2478/v10288-012-0027-0.

Sunardy, E., Kimura, J., 1998. Temporal chemical variations in late Cenozoic volcanic rocks around The Bandung Basin, West Java. Indonesia. J. Min. Petr. Econ. Geol 93, 103–128. https://doi.org/10.2465/GANKO.93.103.

Surmayadi, M., Sumintadireja, P., Irawan, D., Arisbaya, I., 2011. Dinamika vulkanisme Gunung Api Tangkuban Parahu, in: Joint Convention HAGI-IAGI. Makasar. https://doi.org/10.13140/RG.2.1.3527.4088.

Tamrat, W., Rose, J., Grauby, O., Doelsch, E., Levard, C., Chaurand, P., Basile-Doelsch, I., 2019. Soil organo-mineral associations formed by co-precipitation of Fe, Si and Al in presence of organic ligands. Geochim. Cosmochim. Acta 260, 15–28. https://doi.org/10.1016/j.gca.2019.05.043.

Thommes, M., Kaneko, K., Neimark, A.V., Olivier, J.P., Rodriguez-Reinoso, F., Rouquerol, J., Sing, K.S.W., 2015. Physisorption of gases, with special reference to the evaluation of surface area and pore size distribution (IUPAC Technical Report). Pure Appl. Chem. 87, 1051–1069. https://doi.org/10.1515/pac-2014-1117.

Topographical Service Batavia, 1941. Topographical map West Java 1:50,000 (Goenoeng Tangkoebanprahoe).

Uehara, G., Gillman, G., 1981. The mineralogy, chemistry, and physics of tropical soils with variable charge clays. Westview Press Inc, Colorado.

Utami, S.R., Mees, F., Dumon, M., Qafoku, N.P., Van Ranst, E., 2019. Charge fingerprint in relation to mineralogical composition of Quaternary volcanic ash along a climatic gradient on Java Island, Indonesia. Catena 172, 547–557. https://doi.org/10.1016/j.catena.2018.09.024.

Van Bemmelen, R.., 1949. The Geology of Indonesia. Vol. IA: General Geology of Indonesia and Adjacent Archipelagoes. The Hague, Jakarta. https://doi.org/10.1144/gospp.

Van Breemen, N., Mulder, J., Driscoll, C.T., 1983. Acidification and alkalinization of soils. Plant Soil 75 (3), 283–308.

Vander Linden, C., Li, Z., Iserentant, A., Van Ranst, E., de Tombeur, F., Delvaux, B., 2021. Rainfall is the major driver of plant Si availability in perudic gibbsitic Andosols. Geoderma 404, 115295. https://doi.org/10.1016/j.geoderma.2021.115295.

Wagai, R., Mayer, L.M., Kitayama, K., 2009. Extent and nature of organic coverage of soil mineral surfaces assessed by a gas sorption approach. Geoderma 149, 152–160. https://doi.org/10.1016/j.geoderma.2008.11.032.

Wei, C., Ni, J., Gao, M., Xie, D., Hasegawa, S., 2006. Anthropic pedogenesis of purple rock fragments in Sichuan Basin, China. Catena 68, 51–58. https://doi.org/10.1016/j.catena.2006.04.022.

Yu, G., Xiao, J., Hu, S., Polizzotto, M.L., Zhao, F., McGrath, S.P., Li, H., Ran, W., Shen, Q., 2017. Mineral Availability as a Key Regulator of Soil Carbon Storage. Environ. Sci. Technol. 51, 4960–4969. https://doi.org/10.1021/acs.est.7b00305.

Zhang, J., Xiao, J., Li, S., Ran, W., 2017. Manure amendment increases the content of nanomineral allophane in an acid arable soil. Sci. Rep. 7 https://doi.org/10.1038/s41598-017-14445-2.

Zimmerman, A.R., Chorover, J., Goyne, K.W., Brantley, S.L., 2004. Protection of mesopore-adsorbed organic matter from enzymatic degradation. Environ. Sci. Technol. 38, 4542–4548. https://doi.org/10.1021/es035340+.